Interpretation of hard rock seismic data using 3D prestack diffraction imaging

M. Javad Khoshnavaz*
Department of Exploration Geophysics, Curtin University, Perth, Western Australia, and DET CRC
mj.khoshnavaz@postgrad.curtin.edu.au

Andrej Bóna
Department of Exploration Geophysics, Curtin University, Perth, Western Australia, and DET CRC
A.Bona@curtin.edu.au

M. Shahadat Hossain
Department of Exploration Geophysics, Curtin University, Perth, Western Australia, and DET CRC
msh@gmail.com

Milovan Urosevic
Department of Exploration Geophysics, Curtin University, Perth, Western Australia, and DET CRC
M.Urosevic@curtin.edu.au

SUMMARY

Mineral deposits are associated with geological settings characterized by discontinuities and complex structural heterogeneities such as fracture zones, small-scale objects, intrusive and steeply dipping structures. Therefore, detecting such heterogeneities is of primary interest in mineral exploration. Usually, the scale and shape of such heterogeneities cause the seismic energy to diffract rather than reflect. Despite the natural lack of reflectors and potentially abundant number of diffrators, there are only few case studies of diffraction imaging in hard rock environments with almost no examples of diffraction imaging in prestack domain. Herein, we fill this gap by implementing a 3D prestack diffraction imaging technique to detect point diffractors in hard rock environment. The technique includes computation of diffraction traveltime curves followed by semblance analysis along the curves, with high value of semblance corresponding to high diffractivity.

The performance of the method is demonstrated on a 3D synthetic seismic data and applied to a 3D field seismic data set recorded over Kevitsa mineral deposit in the northern Finland. The results of the 3D prestack diffraction imaging method suggest that diffractivity is a powerful attribute that can be used with other seismic attributes for the interpretation of seismic data in hard rock environments.

Key words: Diffraction imaging, interpretation, 3D, hard rock, pre-stack.

INTRODUCTION

The main purpose of seismic imaging is to characterize subsurface geology. Seismic data generated from subsurface structures contains three types of coherent events: reflections, refractions and diffractions. Routine seismic imaging and interpretation techniques, which are mainly designed for soft rock environments, use reflections and refractions with the assumption that the subsurface geology contains a group of smooth interfaces. However, application of such methods may results in failure in hard rock environments, where the geological structures are much more complex with features such as local discontinuities, fracture zones and small scale objects of different shapes. These complexities that can be associated with ore bodies are often smaller than the Fresnel zone associated with the source frequencies and depth of the deposit (Eaton et al. 2003). Therefore, the small scale objects and ore deposit could behave as a prominent seismic diffractions/scatters (Milkereit et al., 2000).

Diffractions are commonly detected by computing coherency of recorded seismic waves along the expected traveltime curves in either post or prestack domains. Diffractions have been employed with different purposes. The importance of diffractions for fault detection was shown by Kery (1952). Trorey (1970) derived the theoretical response of a diffractor in seismic imaging. Harlan et al. (1983), estimated seismic velocities from diffracted waves. Landa and Keydar (1998) used diffractions to detect small objects and discontinuities. Sava et al. (2005) used diffraction imaging in wave-equation migration velocity analysis. Bóna et al. (2013) applied a post stack diffraction imaging technique in hard rock environment. They showed the importance of diffraction imaging to detect small scale objects and local discontinuities in the exploration of mineral deposits. Khoshnavaz et al. (2015) proposed and applied a 2D prestack diffraction imaging method on a hard rock dataset. In hard rock environments, there is often no considerable lateral velocity change and the assumption of waves propagating with a constant effective velocity medium is valid for these environments. In these situations, scattering of seismic energy is due to the relatively large contrast in density (Urosevic et al., 2012). Thus, time imaging is often sufficient for hard rock settings. In this paper, we implement a time-domain 3D prestack diffraction imaging method to a 3D synthetic seismic data and to a 3D field data set that is conducted over Kevitsa mineral deposit, in northern Finland. The focus is to search for point diffractors, coming from fracture zones and wedges of vertical intrusions.

METHODOLOGY

There are two main steps to image diffractions:

- Computation of traveltime curves corresponding to a diffractor at an image point
- Measurement of coherency of the recorded seismic waves along the curves (by using semblance resulting in so-called "D-section").

Diffraction ray path in the source-receiver-offset space for a point diffractor fixed at D, shown in Figure 1, is given by the double-square-root equation for all possible sources and receivers in a seismic survey (Claerbout, 1985)

$$t = \sqrt{\left(\frac{x_D - x_S}{v}\right)^2 + \left(\frac{y_D - y_S}{v}\right)^2 + \frac{{t_0}^2}{4}} + \sqrt{\left(\frac{x_D - x_R}{v}\right)^2 + \left(\frac{y_D - y_R}{v}\right)^2 + \frac{{t_0}^2}{4}}. \tag{1}$$

(x_S, y_S), (x_R, y_R) and (x_D, y_D) denote the horizontal coordinates of sources, receivers and the point diffractor, respectively. v and t_0 are time-imaging velocity and vertical two-way-travel-time, respectively. The stacking velocity (v) can be estimated from the velocity analysis of the reflection data (e.g. constant velocity stack and semblance analysis). Semblance analysis, which is a robust technique in coherency measurement of seismic events, was proposed by Landa and Keydar (1998) to search for the diffracted energy in the recorded seismic data. Semblance formulation, derived by Taner and Kohler (1969), is given by

$$S = \frac{\sum_{t=-m}^{+m} \left(\sum_{i=1}^{N} f_{it}\right)^2}{N \sum_{t=-m}^{m} \sum_{i=1}^{N} {f^2}_{it}}. \tag{2}$$

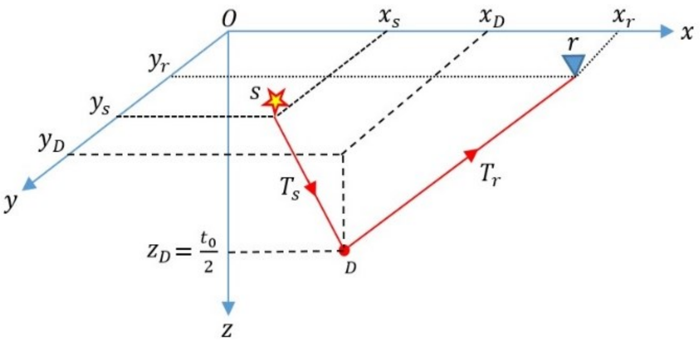

Figure 1: 3D geometry of diffraction ray path, from a seismic source (s) to a diffractor (D), and from the diffractor to the receiver on the surface (r).

where f_{it} is the i^{th} sample at a given time window ($2m$) and N is the number of traces in the selection. The graph of semblance, obtained by scanning all the space of possible diffractors, is called D-section or D-volume.

APPLICATION TO A SYNTHETIC DATA EXAMPLE

In the following example, we applied the prestack diffraction imaging method to a 3D synthetic seismic dataset. The 3D velocity model used to generate the synthetic data was a constant velocity cube with the size of 600×600×700 m^3 including point diffractors at the depth of 350 m (Figure 2a). We used 14400 receivers and 121 shots in the survey (Figure 2b). All receivers were recording during the recording process of each shot. A Ricker wavelet with the dominant frequency of 50 Hz is used for modelling. Sampling interval of 2 ms and geophone spacing of 5 m were chosen to generate the data. We contaminated the recorded data with random noise so that the signal-to-noise ratio is 0.7. Figure 2c shows a part of noisy seismic data from different in-lines.

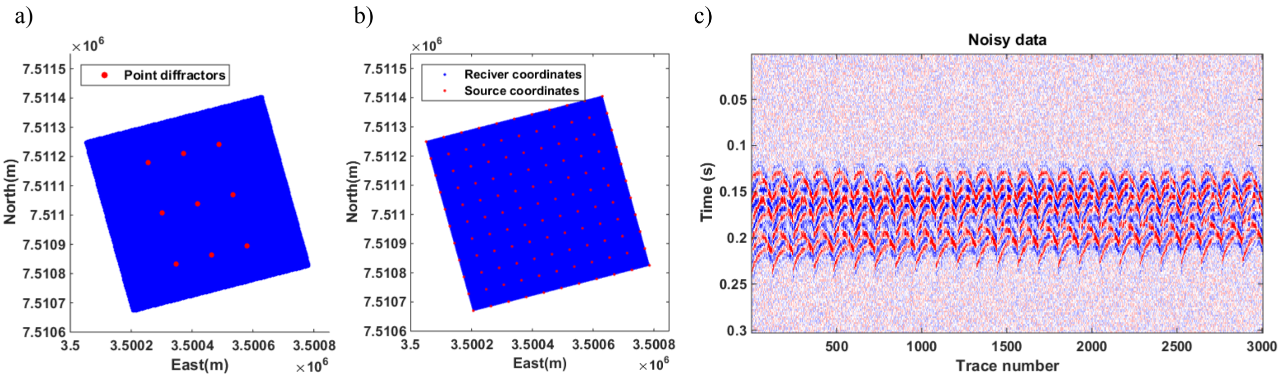

Figure 2. a) Position of point diffractors on the surface located at 350 m/ 0.116 s b) 3D seismic survey used for forward modelling, , and c) part of noisy seismic data from different in-lines for the first shot.

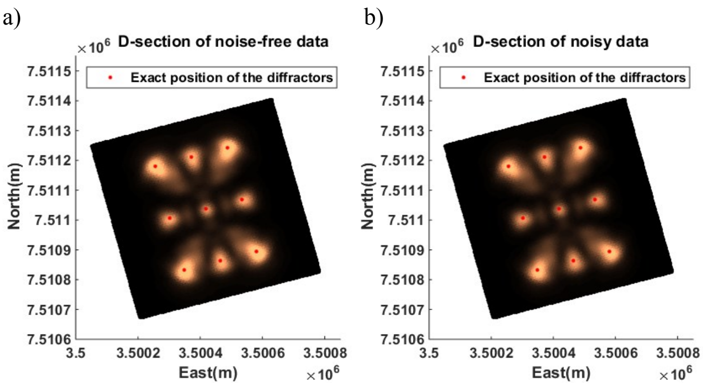

Figure 3. D-section constructed for a) noise-free and b) noisy synthetic data sets. Red dots indicate the exact location of the point diffractors in the target time/depth slice used in forward modelling.

We applied the proposed technique to the noise-free data as well as noisy data. Diffraction traveltime curves were computed using the constant P-velocity of 6000 m/s in the time/depth of the target (350 m/ 0.116 ms) followed by D-section construction through semblance analysis. A time window of 25 samples was used along the computed diffraction travel times. Figure 3a-3b show the D-sections in the target time/depth for the noise-free and noisy data, respectively. Lighter colors indicate higher diffractivity in the D-section. Red dots indicate the exact position of the point diffractors used to generate the data. It is seen that there is a high correlation between them and the highest diffractivities in both D-sections. The negligible contrast between the D-sections constructed for noisy and noise-free seismic data emphasizes on the robustness of semblance analysis in coherency measurement of seismic events in the presence of random noise.

APPLICATION TO A FIELD DATA SET

The proposed 3D pre-stack diffraction imaging technique is applied to a 3D field dataset recorded in 2010 over an area of about 9 km2 at the Kevitsa Ni-Cu-PGE orebody, northern Finland. Figure 4 shows the schematic geologic map of the area and the location of the 3D seismic survey.

According to Rasanen et al. (2001), Mutanen and Huhma (2001), and Koivisto et al. (2012), the Kevitsa Ni–Cu–PGE deposit is a large, low-grade, disseminated sulfide deposit emplaced within layered sedimentary and volcanic rocks of the Central Lapland Greenstone Belt (CLGB) in northern Finland. The intrusion is located just south of the 2.4 Ga old Koitelainen layered intrusion, and west of the Satovaara intrusion. Phyllites and black schists represent the youngest sedimentary rocks found in the area. No reliable ages for the metasediments and metavolcanics are available, however, an approximate age of 2.06 Ga was ascertained by crosscutting the Kevitsa intrusion. In addition, age data from the nearby Rantavaara area indicates that Phyllites are older than 2.15 Ga, and the gabbros of Koitelainen layered intrusion have been dated to be 2.4 Ga old. The oldest rocks in the area are felsic volcanic rocks located in the south of Koitelainen intrusion. The oval–shaped, northeast–southwest trending Kevitsa intrusive complex is characterized by olivine pyroxenite and its altered derivative metaperidotite in the northern part of the intrusion, and by gabbros in the south. The Ni–Cu-–PGE deposit is located in the olivine pyroxenite part of the intrusion (Koivitso et al., 2012).

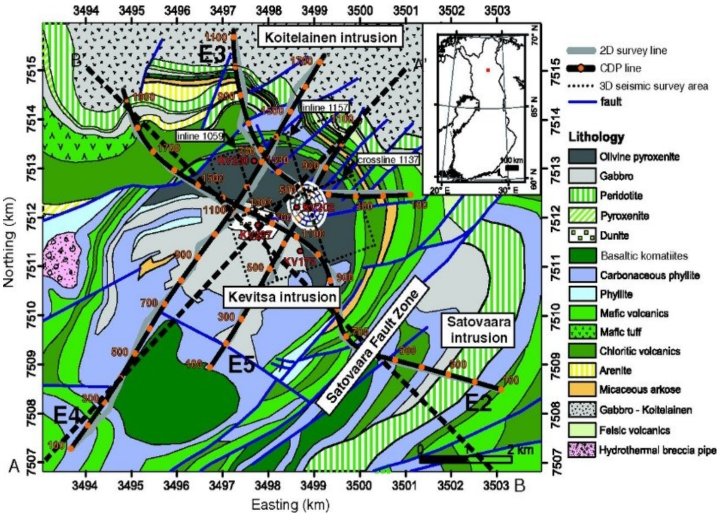

Figure 4: Geological map of the Kevitsa Ni-Cu-PGE deposit, showing the location of the 3D seismic survey (boxed area), deep boreholes in the area and inline and crossline numbers used in this paper (after Koivitso et al., 2012). Note the grey colour indicating Olivine pyraxenite that hosts the mineral deposits indicated by the white contours.

In order to apply the 3D diffraction imaging algorithm, we used the migration velocity field used for prestack time migration (PSTM) by Ziramov et al. (2015). Figure 5a shows the migration velocity for the time slice at 190 ms or equivalently at 570 m, which is within the depth of interest. It is observed that the lateral velocity change, which varies between ±100 m/s, is not considerable in the whole area. Given the migration velocity, diffraction traveltime curves were computed for each image point. Then, semblance analysis was done along the diffraction traveltime curves with the window of 30, to construct the image domain or D-section. Figure 5b shows the D-section computed for the time slice. Lighter colors denote higher values of semblance; the higher the semblance, the higher the diffractivity. To quantify the obtained result, we also used dip-illumination attribute computed at the target depth/time (Figure 5c). This attribute uses a cross-correlation dip estimation method, and the result is a directional view of the calculated dip, where the direction is in degrees and the dip magnitude. Based on the drill-hole data, the metasediments and metavolcanic layers are dipping approximately 50° to 60° to the south in the northern part of the Kevitsa intrusive complex (Koivisto et al. 2012). In the south, the rock layers display a variety of orientations towards north, south, and east, claiming that the rocks were affected by gentle folding (Koivisto et al. 2012). Comparison between the geological map, dip-illumination attribute and diffractivity attribute shows that the higher diffractivity is connected to the Olivine Pyroxenite formation that hosts the mineral deposits. We interpret the high diffractivity associated with the host rock as being generated by highly fractured zones and corresponding tips of mineralization.

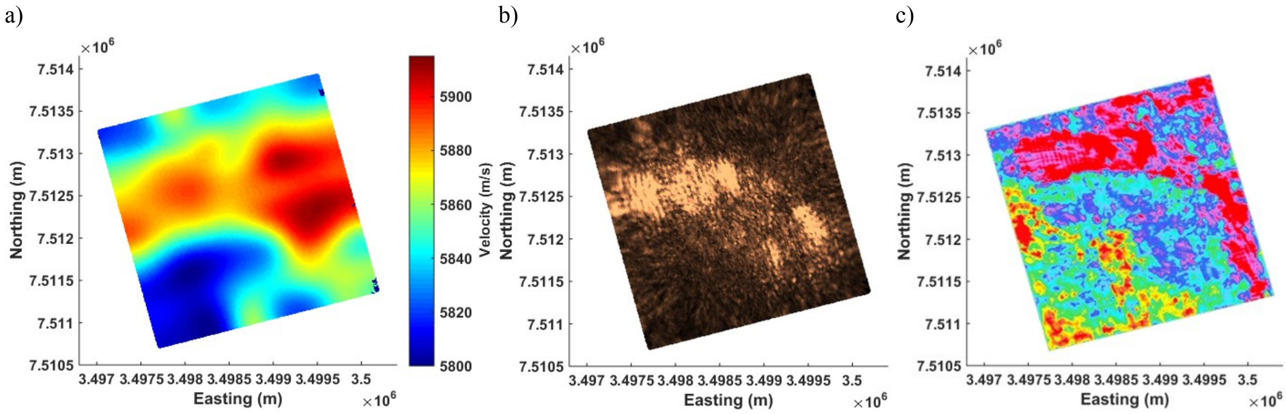

Figure 5: a) The migration velocity field used for PSTM at 190 ms/570 m, b) diffractivity, showing the wedges of the geological features and/or fracture zones, lighter colours indicate higher diffractivity. C) Geological structure boundaries extracted by dip-illumination, different colours indicate different formations.

CONCLUSIONS

To detect small scale objects and non-smooth interfaces such as fracture zones and tips of mineralization that are not imaged by reflection seismic methods, we implemented a 3D prestack diffraction imaging technique to a field data set acquired at Kevitsa, northern Finland. Since the seismic velocity in hard rocks often does not vary significantly, we chose to use time-domain version of the diffraction imaging. The results of the application show an area of strong diffractivity that closely corresponds to the area of Olivine Pyroxenite inferred from borehole data. We attribute this high concentration of diffractors to the tips of mineralization in the fractured Olivine Pyroxenite. This area indeed contains the location of the planned mine. We believe that we have demonstrated usefulness of conceptually simple time-domain diffraction imaging to map geological features that are often very important for the exploration of mineral deposits in hard rock environments.

ACKNOWLEDGMENTS

The work has been supported by the Deep Exploration Technologies Cooperative Research Centre whose activities are funded by the Australian Government's Cooperative Research Centre Program. Authors would like to appreciate First Quantum Minerals Ltd. for providing the 3D seismic hard rock dataset and for permission to publish the results.

REFERENCES

Bóna, A., R. Pevzner, K. Tertyshnikov, A. Greenwood, B. Sun, S. Yavuz, and M. Urosevic, 2013, Diffraction Imaging in Hard-rock Environments: 75th EAGE Conference & Exhibition incorporating SPE EUROPEC, DOI: 10.3997/2214-4609.20130702.

Claerbout, J. F., 1985, Imaging the earth's interior: Blackwell Scientific Publications, 163-165.

Eaton, D.W., 1999, Weak Elastic-Wave Scattering from Massive Sulfide Orebodies: Geophysics, 64, no. 1, 289-299.

Harlan, W. S., J. F. Claerbout, and F. Rocca, 1983, Extracting velocities from diffractions: Annual SEG Meeting, Expanded Abstracts, vol. 2, no. 1, pp. 574-577.

Khoshnavaz, M. J., A. Bóna, M. Urosevic, S. Ziramov and P. Ahmadi, 2015, Pre-stack diffraction imaging and its application in hard rock environment, Accepted in the 77th EAGE Conference & Exhibition.

Koivisto, E., A. Malehmir, P. Heikkinen, S. Heinonen, and I. Kukkonen, 2012, 2D reflection seismic investigations at the Kevitsa Ni-Cu-PGE deposit, northern Finland: Geophysics 77, no. 5, WC149-WC162.

Krey, T., 1952, The significance of diffraction in the investigation of faults: Geophysics 17, no. 4, 843-858.

Landa, E., and S. Keydar, 1998, Seismic monitoring of diffraction images for detection of local heterogeneities: Geophysics 63, no. 3, 1093-1100.

Milkereit, B., E.K. Berrer, A.R. King, A.H. Watts, B. Roberts, E. Adam, D.W. Eaton, J. Wu, and M.H. Salisbury, 2000, Development of 3−D Seismic Exploration Technology for Deep Nickel-Copper Deposits-a Case History from the Sudbury Basin, Canada: Geophysics, 65, 1890-1899.

Mutanen, T., and H. Huhma, 2001, U-Pb geochronology of the Koitelainen, Akanvaara and Keivitsa layered intrusions and related rocks: SPECIAL PAPER-GEOLOGICAL SURVEY OF FINLAND, 229-246.

Rasanen, J., H. Huhma, J. Risinen, and H. Huhma, 2001, U-Pb datings in the Sodankyla schist area, central Finnish Lapland: SPECIAL PAPER-GEOLOGICAL SURVEY OF FINLAND, 153-188.

Sava, P. C., B. Biondi, and J. Etgen, 2005, Wave-equation migration velocity analysis by focusing diffractions and reflections: Geophysics 70, no. 3, U19-U27.

Taner M.T., and M. Koehler, 1969, Velocity spectra-digital computer derivation applications of velocity functions: Geophysics, 34, no. 6, 859-881.

Trorey, A. W., 1970, A simple theory for seismic diffractions: Geophysics 35, no. 5, 762-784.

Urosevic M., G. Bhat, and M.H. Grochau, 2012, Targeting nickel sulfide deposits from 3D seismic reflection data at Kambalda, Australia: Geophysics, 77, no. 5, WC123–WC132.

Zhang, J., and J. Zhang, 2014, Diffraction imaging using shot and opening-angle gathers: A prestack time migration approach: Geophysics 79, no. 2, S23-S33.

Ziramov, S., A. Dzunic, and M. Urosevic, 2015, Kevitsa Ni-Cu-PGE deposit, North Finland, A seismic case study: Annual ASEG Meeting, Expanded Abstracts, no. 1, 1-4.